arXiv:cond-mat/0201128v1 [cond-mat.stat-mech] 9 Jan 2002

# Monte-Carlo simulation of nucleation in the two-dimensional Potts model

S.B. Rutkevich *
*Institute for Theoretical Physics,*
*University of Cologne, D-50937 Köln, Germany*
*e-mail: rut@mailaps.org*

March 22, 2022

**Abstract**

Nucleation in the two-dimensional $q$-state Potts model has been studied by means of Monte-Carlo simulations using the heat-bath dynamics. The initial metastable state has been prepared by magnetic quench of the ordered low-temperature phase. The magnetic field dependence of the nucleation time has been measured as the function of the magnetic field for different $q$ and lattice sizes at $T = 0.5\,T_c$. A size-dependent crossover from the coalescence to nucleation region is observed at all $q$. The magnetic field dependence of the nucleation time is roughly described by the classical nucleation theory. Our data show increase of the anisotropy in the shape of the critical droplets with increase of $q$.

**KEY WORDS:** Potts model, nucleation, metastable state, critical droplet, Monte-Carlo simulations.

## 1 Introduction

Nucleation of 'bubbles' or 'droplets' of the stable phase is a very common phenomenon which initiates relaxation of metastable states near the first order phase transition in many systems of condensed matter physics [1], quantum fields [2], and cosmology [3, 4]. The main quantity of interest for the theory and applications is the nucleation time, which characterizes the time required by the system to leave the metastable state. In lack of

*On leave from: Institute of Solid State and Semiconductor Physics, P. Brovka str. 17, Minsk 220072, Belarus.

a consistent theory of the metastability, the nucleation problem has been subjected to extensive study in computer simulations. Numerical data are usually interpreted in terms of the phenomenological classical nucleation theory, or in terms of its field-theoretical version proposed by Langer [5]. A great deal of this work has been carried out on the Ising model supplied with some appropriate dynamics.

It seems reasonable, however, to extend the numerical study of the nucleation to more complex and rich models, taking into account a great variety of physical realizations of this phenomenon. In this paper, we have studied nucleation in the two-dimensional $q$-state Potts model by use of the Monte-Carlo simulation. Due to a rich equilibrium phase structure, this model provides a lot of possibilities to form the initial metastable phase. For $q > 4$, the zero-field Potts model has the first order phase transition point driven by the temperature [7]. Near this point, the metastable state can be prepared by a quenched cooling from the high to low temperature phase. Relaxation of such a state in different regimes has been studied numerically by Safran *et. al* [8, 9], and by Arkin *et. al* [10, 11]. Meunier and Morel [12] analysed metastability in the thermally quenched Potts model within the Fisher's droplet picture approach [13]. Arkin *et. al* confirmed [10, 11], that in a case of slight quench (small $|T_c - T|$), the equilibrium proceeds through the usual nucleation mechanism. However, lack of the macroscopic order parameter (like the average magnetization in the Ising system below $T_c$) in the both initial and final states hinders precise measurement of the nucleation time in this regime.

We simulate relaxation of the metastable states, which are induced in the Potts ferromagnet near the first order phase transition driven by the external magnetic field $H$. The heat-bath dynamics is used to thermalize spins. Nucleation time is measured as the function of the applied field at $T = 0.5\,T_c$ for $q = 2, 3, 5, 15$.

One can say, that for small $q$ , $q \leq 4$, the line $H = 0, \quad 0 < T < T_c$ in the Potts model represents the liquid-vapour phase transition, and it simulates the liquid-solid transition for large $q$, $q > 4$. It should be noted, that the Langer's theory of nucleation [5] based on the coarse-grained free-energy functional can not be applied in the latter case [14]. So, our aim is to identify in the Potts model the nucleation regimes well-known in the Ising model, and to study how they are modified by increase of $q$.

## 2 The Potts Model

We study the $q$-state ferromagnetic Potts model on the square lattice having $L$ rows and $L$ columns. The discrete spin variable $\sigma = 1, 2, ..., q$ is associated with each lattice site $j$. Helical boundary conditions are used [6]. The model Hamiltonian is defined as

$$\mathcal{E} = -2J \sum_{<i\,j>} \delta(\sigma_i, \sigma_j) - H \sum_j \delta(\sigma_j, 2). \tag{1}$$

Here the first summation is over the nearest neighbour pairs, $2J > 0$ is the coupling constant, $H$ is the external magnetic field applied along the 2-direction, and

$$\delta(\sigma, \sigma') = \begin{cases} 1 & \text{if } \sigma = \sigma', \\ 0 & \text{if } \sigma \neq \sigma'. \end{cases}$$

We use also dimensionless parameters $K = J\beta$, and $h = H\beta$, where $\beta = 1/k_B T$ is the inverse temperature. The macroscopic state of the lattice can be described by $q$ real positive order parameters $M(\sigma)$

$$M(\sigma) = L^{-2} \sum_j \delta(\sigma_j, \sigma), \tag{2}$$

$$\sum_{\sigma=1}^{q} M(\sigma) = 1.$$

The model undergoes ferromagnetic phase transition at the critical temperature

$$T_c = \frac{2J}{k_B \log(1 + \sqrt{q})}. \tag{3}$$

The ferromagnetic low-temperature phase at zero field is $q$-times degenerated. Different ferromagnetic phases are enumerated by the discrete parameter $\hat{\sigma}$. This implies that in the $\hat{\sigma}$-phase, the orientation $\hat{\sigma}$ dominates in the lattice. For a review of many others known properties of the Potts model see [15].

# 3 Classical Nucleation Theory

The classical nucleation theory (CNT) considers thermally induced generation of the stable phase droplets in the metastable surrounding. A droplet of radius $R$ can appear with probability $p(R)$ proportional to the Boltzmann factor

$$p(R) \sim L^2 \, \exp[-\beta \mathcal{F}(R)],$$

where $\mathcal{F}(R)$ is the droplet free energy[1]:

$$\mathcal{F}(R) = 2\pi R \, s - \pi R^2 M \, H. \tag{4}$$

Here $s$ is the surface tension on the droplet boundary, $M$ is the zero-field spontaneous magnetization. The critical droplet radious $R_c$ maximizes the free energy (4). It is postulated in CNT, that the nucleation time $t(h, L)$ is inversely proportional to the probability of generation of the critical droplet:

$$t(h, L) \sim L^{-2} \exp[\beta \mathcal{F}(R_c)] = L^{-2} \exp[\pi(\beta s)^2/(M \, h)]. \tag{5}$$

[1] In the Ising model, the volume free energy $-2\,\pi R^2 M \, H$ of the droplet has an additional factor 2 due to a different definition of the magnetic field $H$.

The classical nucleation theory considers only spherical droplets. This is reasonable, if the surface tension of the domain wall does not depend on its is orientation. If the surface tension is anisotropic, the critical droplet are supposed to have the equilibrium shape given by the Wulff's construction [1]. In this case equation (5) should be modified to

$$t(h, L) \sim L^{-2} \exp[A(T)/h], \tag{6}$$

where the amplitude $A(T)$ is determined by the equilibrium droplet shape. In the Ising model, this shape is given by the equation [17]

$$\cosh x_1 + \cosh x_2 = \sinh(2K) + \frac{1}{\sinh(2K)}, \tag{7}$$

where $x_1$, $x_2$ denote Descartes coordinates on the droplet boundary. It varies from circle at $T = T_c - 0$ to square at $T = 0$.

The amplitude $A(T)$ can be written as $A(T) = S(T)/M$, where $S(T)$ denotes the area bounded by the curve (7), and

$$M = \{1 - [\sinh(2K)]^{-4}\}^{1/8}.$$

Numerically we have for the $q = 2$ state Potts (Ising) model at $T = 0.5\, T_c$:

$$\begin{aligned} S(0.5\, T_c) &= 6.537,\ M(0.5\, T_c) = 0.998, \\ A(0.5\, T_c) &= 6.55. \end{aligned} \tag{8}$$

It should be noted, that equation (6) gives only the leading $h \to 0$ asymptotics of the nucleation time. The most important correction is expected to have the form of the prefactor with a power-law $h$-dependence [1]

$$t(h, L) = L^{-2} \frac{B(T)}{h^{b+c}} \exp[A(T)/h]. \tag{9}$$

The exponent $b$ here arises in the field theoretical nucleation theory from the contribution of the capillary waves on the critical droplet surface [18], $b = 1$ in the two-dimensional Ising model. The exponent $c$ gives the $h$ variation of the so-called kinetic prefactor, which depends on the chosen dynamics. For dynamics which can be described by the Fokker-Plank equation, the value $c = 2$ is expected [19, 20].

The exact equilibrium (Wulff's) shape of the droplet is not known for the Potts model with $q \geq 3$. So, we had to use more simple and less accurate estimates for the amplitude $A(T)$. We have used square and circle approximations for the critical droplet shape. The surface tension in the both cases was replaced by its zero-temperature value $s = 2J$. This yields for the amplitude $A(T)$ in the nucleation time exponent:

$$A(T) = \begin{cases} 16\, K^2, & \text{for square droplet,} \\ 4\pi\, K^2. & \text{for circle droplet} \end{cases} \tag{10}$$

Table 1: Amplitude $A(T)$ at $T = 0.5\,T_c$ for square and circle droplets.

| q | $A(0.5\,T_c)$ | |
|---|---|---|
| | square | circle |
| 3 | 16.2 | 12.7 |
| 5 | 22.1 | 17.3 |
| 15 | 40.1 | 31.5 |

Numerical values for the amplitude $A(T)$ calculated from (10) for different $q$ at $T = 0.5\,T_c$ are given in Table 1.

The size-dependent behaviour (6) of the nucleation time is observed in not very large lattices, in the so-called nucleation regime. In this regime, only one droplet of the stable phase appears in the system, and then expands to the whole lattice.

At large $L$, the coalescence regime is realized. In this regime the relaxation time does not depend on $L$. Many critical droplets appear in the system, expand and coalesce.

It is expected from the Kolmogorow-Johnson-Mehl-Avrami theory [16], that

$$t(H) \sim \exp[A(T)/(3h)] \tag{11}$$

in the coalescence regime in two-dimensional systems .

# 4 Simulation Scheme

In the Potts model, the applied field and the initial metastable configuration of spins in the lattice can be chosen in many different ways. We have studied only two of them.

- **First regime**. A positive magnetic field $H > 0$ is applied along the 2-direction, whereas all the spins are initially oriented along the 1-directions: $\sigma_j = 1$. Such a field removes completely degeneracy of the low temperature phase, leaving only one equilibrium ferromagnetic state: $\hat{\sigma} = 2$.

- **Second regime**. A negative magnetic field $H < 0$ is applied along 2-direction, and all spins are initially oriented in the same direction $\sigma_j = 2$. The ferromagnetic phase still remains $(q-1)$-times degenerated (if $q \geq 3$) in such a field. In this regime, the system moves to some bifurcation point, and then relaxes to one of the equivalent $(q-1)$ equilibrium states.

The heat-bath technique (Glauber kinetics) has been used to orient the spins. To produce a sequence of pseudorandom numbers, we have used the standard generator of pseudo-random numbers with multiplication by 16807 to give 64-bit integers. The candidate

spins to flip have been chosen sequentially: site by site in the row, and row by row in the lattice. We define the nucleation time $t$ as the number of sweeps through the lattice after which the number of spins in the initial (metastable) phase reduces to $0.5L^2$. The $h$-dependence of the nucleation time $t$ has been measured at $L = 31$, and $L = 1001$. In the nucleation regime, the nucleation time fluctuates very much. So, we had to average the nucleation time in this regime over 100 or even 1000 runs. It is important to note, that for $q \geq 3$ the relation between the nucleation time $t$ and the total relaxation time $t_0$ is not straightforward and is different in different regimes.

A typical time dependence of the order parameters $M(\sigma)$ in the first nucleation regime for $q = 3$ is shown in Fig. 1. Since the fall of the magnetization $M(1)$ is very rapid compared with the time which the system has spent in the metastable state, the nucleation time $t$ and the total relaxation time $t_0$ are essentially the same in this regime. This is true also in the second nucleation regime. In the latter case, however, the system can fall with equal probabilities to one of the equilibrium states, either $\hat{\sigma} = 1$, or $\hat{\sigma} = 3$.

Fig. 2 shows a typical time evolution of the magnetization in the first coalescence regime. Up to the saturation at 1, the magnetization $M(2)$ increases approximately linearly with time due to the steady expansion of many stable phase droplets. Thus, the system reaches equilibrium in about two nucleation times: $t_0 \simeq 2\,t$.

The situation is quite different in the second coalescence regime, see Fig. 3. In this case many critical droplets of the both equilibrium phases $\hat{\sigma} = 0$ and $\hat{\sigma} = 1$ are initially generated in the lattice. They expand and expel the metastable $\hat{\sigma} = 2$ phase from the system in about two nucleation times. The resulting state is still far from the equilibrium, since the lattice is divided into domains of two stable phases $\hat{\sigma} = 1$ and $\hat{\sigma} = 3$. During the final (very slow at low temperatures) stage of the relaxation, these two phases compete, until one of them will expel another from the system. So, the nucleation time $t$ and the total relaxation time $t_0$ may be of different order of magnitude in the second coalescence regime.

# 5 Results

Our simulations were restricted to the temperature $T = 0.5\,T_c$ and the lattice sizes $L = 31$ and $L = 1001$. We have started from the $q = 2$ Potts model, which is equivalent to the Ising model. This provides a good possibility to verify efficiency of the applied simulation scheme, since nucleation in the Ising model has been thoroughly studied [1, 21, 22, 23, 24].

Figure 4 shows the nucleation time in the logscale for the $q = 2$ Potts (Ising) model. Pluses correspond to the nucleation time averaged over 1000 runs in the $L = 31$ lattice. Stars relate to the nucleation time in the $L = 1001$ lattice. Crosses indicate the dispersion $D[t]$ of the nucleation time distribution in the $L = 31$ lattice:

$$D[t] = (\langle t^2 \rangle - \langle t \rangle^2)^{1/2},$$

where $\langle ... \rangle$ denotes averaging over different runs.

Three relaxation regimes are clearly identified: the strong field regime (SFR), the coalescence regime (CR), and the nucleation regime (NR). Increase of the lattice size does not change the nucleation time in the strong field and coalescence regimes. The nucleation regime was not observed in the $L = 1001$ lattice in the studied region of fields $h$. In the nucleation regime, the nucleation time fluctuates very much, and the distribution $p(t)$ of these fluctuations is described by the simple exponential law:

$$p(t) = \frac{1}{\tau} \exp(-t/\tau). \tag{12}$$

For this distribution, the averaged time equals to the dispersion: $\langle t \rangle = D[t] = \tau$. This is indeed observed in the $L = 31$ lattice at $1/h > 1.15$ indicating well established nucleation regime in this field region. The theoretical prediction for the averaged nucleation time in the nucleation regime with the Wulff's shape droplet is given by equation (9), where $b + c = 3$, and $A = 6.55$. The upper straight line in Fig. 4 shows the nucleation theory exponent, and the second (curved) line plots the the same exponent corrected by the prefactor $Ch^{-3}$, i.e. equation (9). Though the latter curve contains only one free parameter - the constant factor $C$ - it fits well the numerical simulation points for the $L = 31$ lattice in the nucleation regime, much better then the first (straight) line.

The curved line gives also a good fit for the dispersion points in the small $L = 31$ lattice not only in the nucleation region, but also at crossover to the coalescence regime down to $h^{-1} \approx 0.8$. The possible explanation of this result may be the following. Measured nucleation time $t$ consists of two terms $t = t_n + t_e$, which have the same order of magnitude in the crossover region. The first term relates to the time of nucleation of the first critical droplet in the system, and the second term denotes the time of the expansion of this droplet to 1/2 of the whole lattice. The first term should strongly fluctuate according to the exponential law (12). If the second term $t_e$ fluctuates much weaker, one should have for the total time dispersion:

$$D[t] = D[t_n + t_e] \approx D[t_n] = \langle t_n \rangle = \tau,$$

where the averaged time $\tau$ of the first droplet nucleation is still given by equation (9). Thus, in the crossover region, dependence (9) should fit better the time dispersion points $D[t]$, than the averaged time $\langle t \rangle$, which is indeed observed.

The first numerical verification of the magnetic field dependence of the prefactor in (9) for the two-dimensional Ising model has been reported by Rikvold *et. al* [22]. In this work, the value $b + c = 3$ was confirmed at $T = 0.8\, T_c$ for the Metropolis dynamics with randomly chosen sites. However, a smaller value $b + c \approx 2$ was observed in [22], when the sites in the lattice were chosen sequentially. Though we have also used the sequential chose of sites in the lattice, our data for the nucleation time in the nucleation region are better fitted by (9) with the prefactor exponent $b + c = 3$, rather then $b + c = 2$, see Fig.

5. This is more clear for the dispersion $D[t]$ (crosses in Fig. 5), since the latter is still described by (9) at the crossover to the coalescence regime.

The lower straight line is the best linear fit for the nucleation time in the larger $L = 1001$ lattice in the coalescence regime (CR). The ratio of slopes $R = 1.9$ of two straight lines in Fig. 4 corresponding to the nucleation and coalescence regimes is much smaller than 3, expected from the theory in the small $h$ limit. However, we are still far from the well-established small $h$ limit, as it is evident from the considerable difference between first and second lines in Fig. 4. If one takes this into account, this disagreement of the observed $R = 1.9$ value with 3 expected in the $h \to 0$ limit becomes not so surprising.

Figures 6-10 show the observed dependence of the nucleation time on the inverse field $h^{-1}$ in the $q = 3, 5, 15$ Potts models, $L = 31, 1001$ in the first $h > 0$ and second $h < 0$ regimes. Pluses correspond to the nucleation time averaged over 100 runs in the smaller lattice. Crosses indicate nucleation time in the $L = 1001$ lattice. Only the second regime $h < 0$ has been studied in the $q = 15$ Potts model, since the nucleation time in the first regime $h > 0$ becomes too long in this case, see equation (13) below.

Qualitatively, the magnetic field dependence of the nucleation time in all cases is similar to that in the Ising model. The same three field regions (SRF, NR, CR) have been observed. As in the Ising case, the nucleation regime was realized only in the smaller lattice, $L = 31$. In the latter regime, the relaxation time strongly fluctuates.

In all cases, $\log\langle t\rangle$ behaves linearly with $1/h$ in the nucleation regime (NR), in agreement with the classical nucleation theory. In the $q = 3$ and $q = 5$ systems the observed slopes ($\log\langle t\rangle$ vs. $h^{-1}$ ) in NR agree with the circle shape of the critical droplets. However, in the $q = 15$ model our data indicate the square critical droplet shape, see Fig. 10 , and Table 1.

The ratio of slopes in nucleation and coalescence regimes varies from $R = 2.6$ in the $q = 3$, $h > 0$ case, down to $R = 2.1$ in the $q = 5$, $h < 0$ case. As in the $q = 2$ model, these values are lower than 3 predicted by the theory.

In the first nucleation regime ($h > 0$), the nucleating critical droplet should be of the single equilibrium phase $\hat{\sigma} = 2$, whereas in the second nucleation regime ($h < 0$), a critical droplet of either of $(q - 1)$ equilibrium phases $\hat{\sigma}$, $\hat{\sigma} \neq 2$ provides relaxation. So, it is naturally to expect, that nucleation time $\langle t_1\rangle$ in the first nucleation regime will be longer, that the nucleation time $\langle t_2\rangle$ in the second nucleation regime, and

$$\frac{\langle t_1\rangle}{\langle t_2\rangle} \approx q - 1. \tag{13}$$

The observed ratios $\langle t_1\rangle/\langle t_2\rangle$ determined from the circle droplet fits in Fig. 6-9

$$\frac{\langle t_1\rangle}{\langle t_2\rangle} \approx \begin{cases} \exp(-2.95)/\exp(-3.64) = 2.0 & \text{for } q = 3, \\ \exp(-1.29)/\exp(-2.8) = 4.5 & \text{for } q = 5 \end{cases} \tag{14}$$

are in a good agreement with (13).

# 6 Summary

We have simulated nucleation in the $q$-state Potts model on the square lattice for $q = 2, 3, 5, 15$. The magnetic field dependence of the nucleation time have been measured in two regimes ($h > 0$ and $h < 0$) at $T = 0.5\,T_c$ for two lattice sizes $L = 31$ and $L = 1001$. The strong field regime, coalescence regime, and nucleation regime are clearly identified.

The observed magnetic field dependencies of the nucleation time is in agreement with the classical nucleation theory, if one takes into account the anisotropy of the critical droplet shape. Our numerical data indicate, that the shape of the critical droplet changes from (roughly) circle towards square with increasing $q$ at the fixed temperature $T = 0.5\,T_c$. A similar result was observed by Bikker *et. al* [25] in numerical calculations of the equilibrium crystal shape in the three-dimensional Potts model. So, increase of $q$ has a similar effect on the equilibrium droplet shape, as decrease of temperature. This is natural, since the both reduce the correlation length, which should increase anisotropy in the system.

The ratio of $(\log(t)\,\mathrm{vs.}\,h^{-1})$ slopes in nucleation and coalescence regimes does not approach 3, predicted by the theory in the $h \to 0$ limit. We associate this discrepancy with the 'finite-$h$ corrections', which are still considerable in the studied region of the magnetic field.

Though $q = 2, 3$ and $q = 5, 15$ state Potts models have different type phase transitions at $T_c$ (continuous for $q = 2, 3$ and first order for $q = 5, 15$), metastable phases in these models relax to the equilibrium in a similar way.

## Acknowledgments

I am grateful to Kurt Binder for suggesting the subject of this work. I am thankful to Dietrich Stauffer for many helpful discussions, and for introducing into computer simulations.
This work is supported by the Deutscher Akademischer Austauschdienst (DAAD) and by the Fund of Fundamental Investigations of Republic of Belarus.

# References

[1] P.A. Rikvold and B.M. Gorman, in *Annual Review of Computational Physics I*, D. Stauffer ed., (World Scientific, Singapore, 1994).

[2] H.E. Stanley, *Introduction to Phase Transitions and Critical Phenomena,* (Clarendon Press, Oxford, 1971).

[3] A.H. Guth, *The Inflationary Universe*, (Addison Wesley, Reading, Mass., 1997).

[4] H.A. Kastrup, Phys. Letters B **419**, 40 (1998).

[5] J.S. Langer, Ann. Phys. (N.Y.) **41**, 108 (1967).

[6] M.E.J. Newman and G.T. Barkema, *Monte-Carlo Methods in Statistical Mechanics* (Clarendon Press, Oxford, 1999).

[7] R.J. Baxter, J. Phys. C **6**, L445 (1973).

[8] S.A. Safran, P.S. Sahni, and G.S. Grest, Phys. Rev. B **28**, 2693 (1983).

[9] P.S. Sahni, D.J. Srolovitz, G.S. Grest. M.P. Anderson, and S.A. Safran, Phys. Rev. B **28**, 2705 (1983).

[10] H. Arkin, T. Celik, B.A. Berg, and H.Meyer-Ortmanns, Int. J. Mod. Phys. C **10**, 1261 (1999).

[11] H. Arkin, T. Celik, Int. J. Mod. Phys. C **11**, 1313 (2000).

[12] J.L. Meunier, and A.Morel, Eur. Phys. J. B **13**, 341 (2000).

[13] M.E. Fisher, Physics (N.Y.) **3**, 255 (1967).

[14] J.D. Gunton, M.San Miguel, and P.S. Sahni *The Dynamics of First order Phase Transitions* in *Phase Transitions and Critical Phenomena*, Vol.8, C.Domb and J.L. Lebowitz eds., (Academic Press, London, 1983).

[15] F.Y. Wu, Rev. Mod. Phys. **54**, 235 (1982).

[16] K. Sekimoto, Int. J. Mod. Phys. B **5**, 1843 (1991).

[17] R.K.P. Zia and J.E. Avron, Phys. Rev. B **25**, 2042 (1982).

[18] N.J. Günther, D.A. Nicole, and D.J. Wallace, J. Phys. A **13**, 1755 (1980).

[19] J.S. Langer, Phys. Rev. Lett. **21**, 973 (1968).

[20] J.S. Langer, Ann. Phys. (N.Y.) **54**, 258 (1969).

[21] D. Stauffer, A. Coniglio, D.W. Heermann, Phys. Rev. Lett. **49**, 1299 (1982).

[22] P.A. Rikvold, H. Tomita, S. Miyashita, and S.W. Sides, Phys. Rev. E **49**, 5080 (1994).

[23] S.Wonczak, R. Strey, D. Stauffer, J. Chem. Phys. **113**, 1976 (2000).

[24] M. Acharyya, D. Stauffer, Eur. Phy. J. B **5**, 571 (1998).

[25] R.P. Bikker, G.T. Barkema, and H. van Beijeren, cond-mat/0011336 (2000).

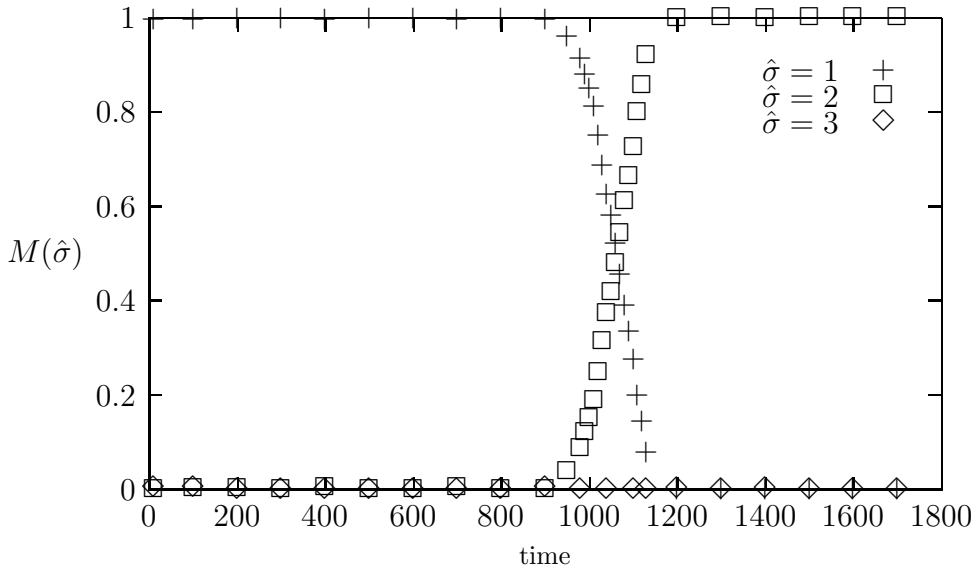



Figure 1: Decay of metastable state in first nucleation regime

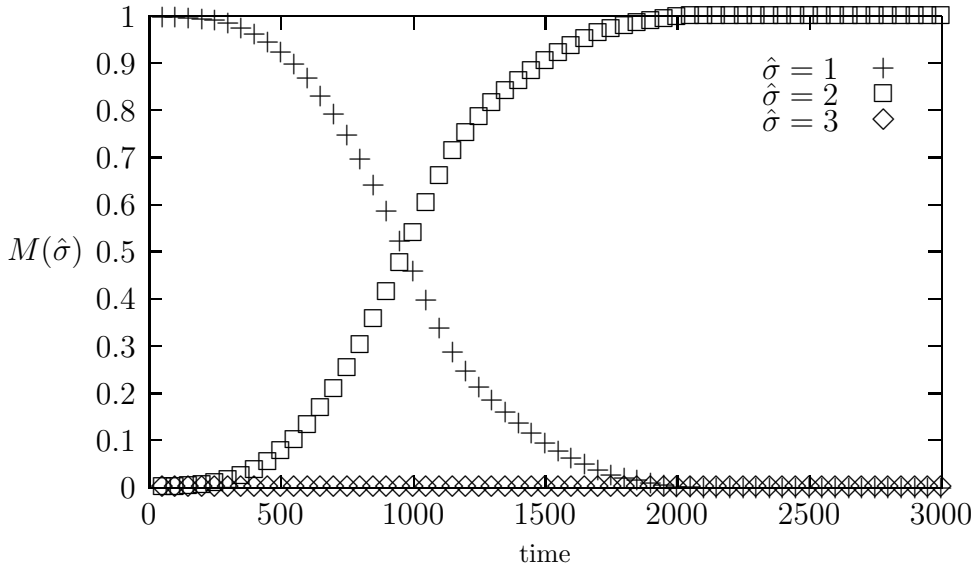



Figure 2: Decay of metastable state in first coalescence regime

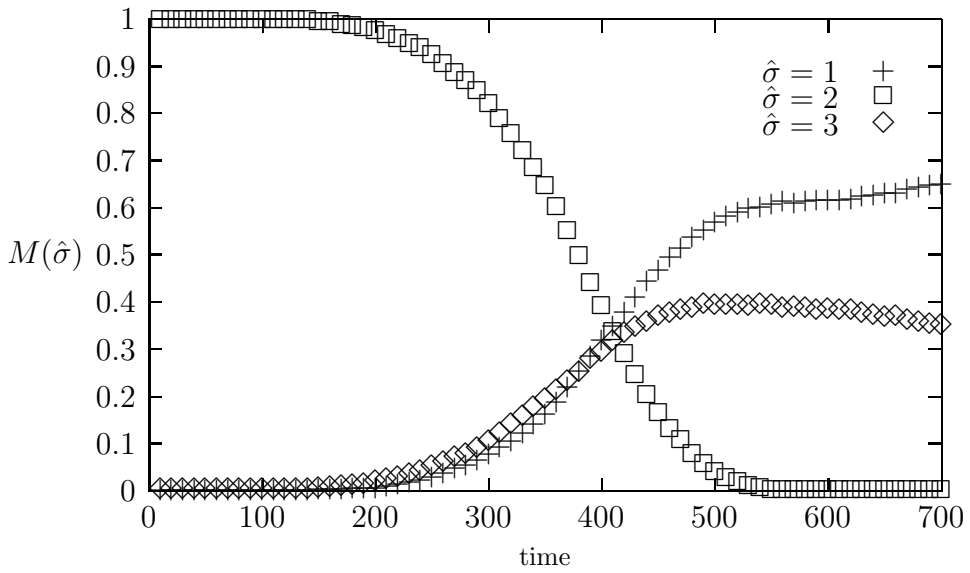



Figure 3: Decay of metastable state in second coalescence regime

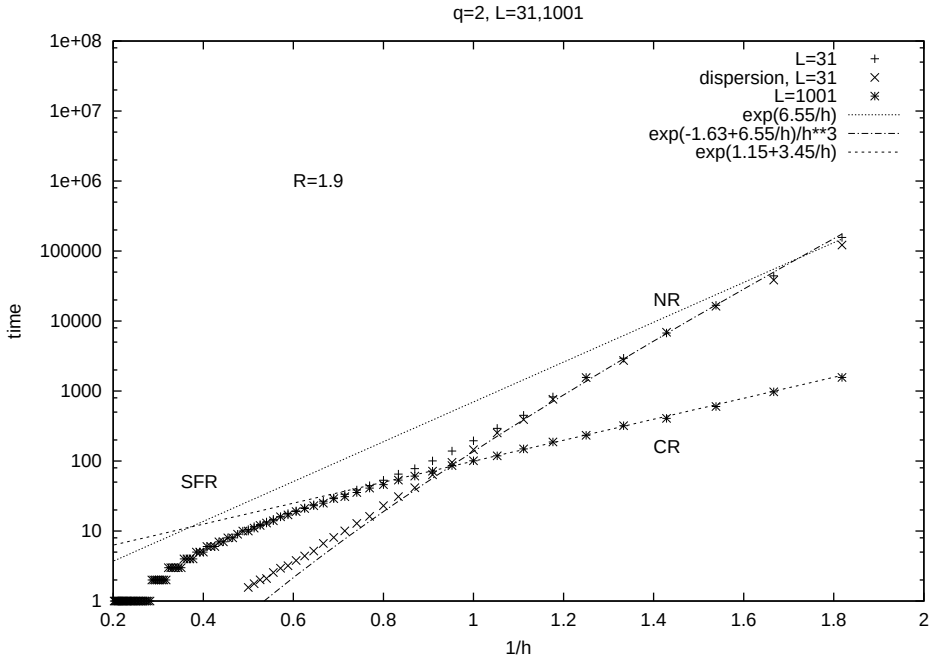



Figure 4: Nucleation time and dispersion plotted against $1/h$ in the $q = 2$ Potts (Ising) model for $L = 31$

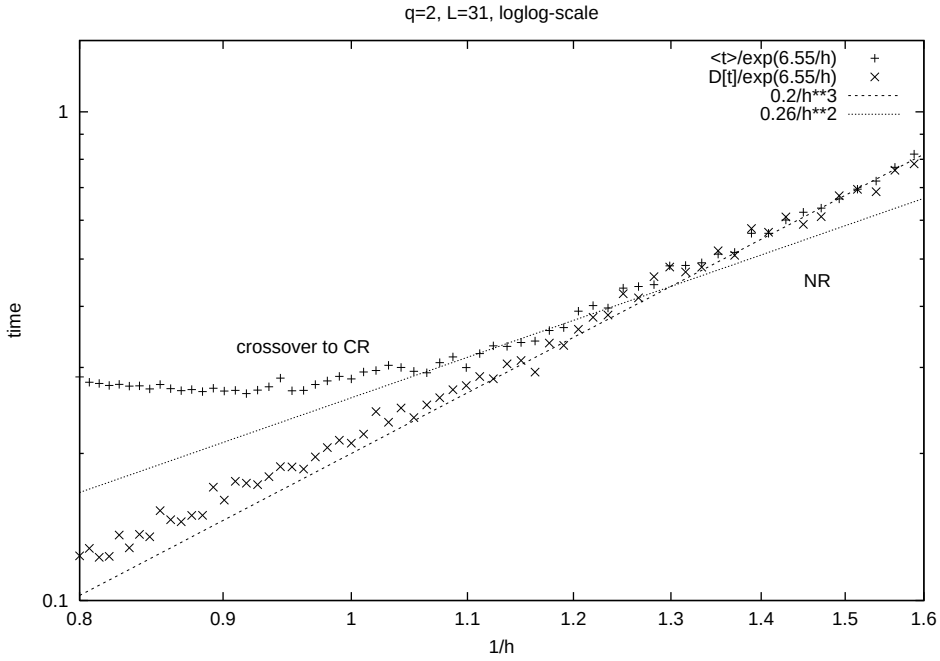



Figure 5: Averaged nucleation time $\langle t \rangle$ and dispersion $D[t]$ divided by $\exp[6.55/h]$, versus $1/h$ (loglog-scale) in the $q = 2$ Potts (Ising) model.

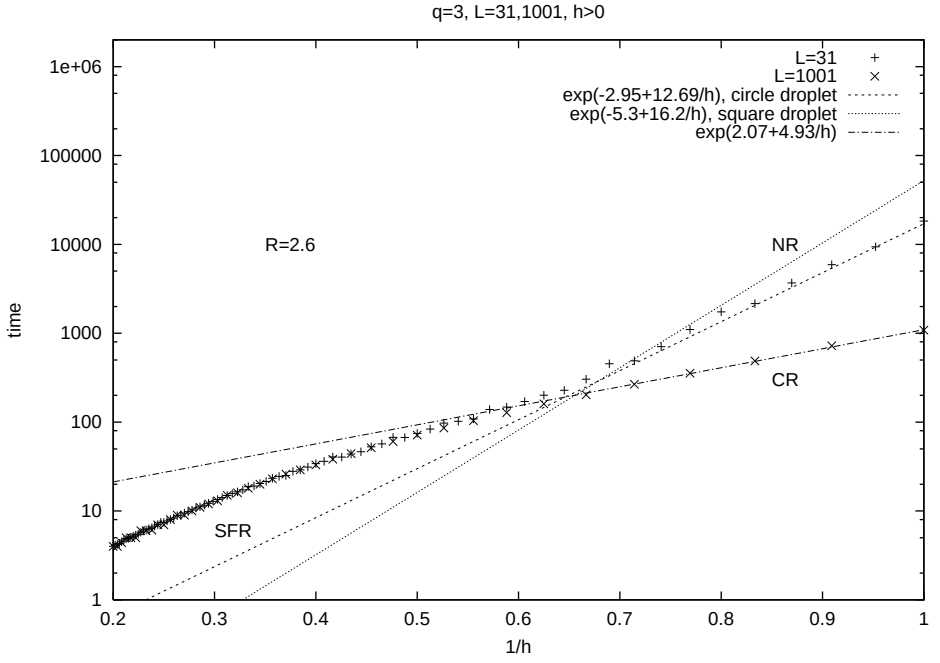



Figure 6: Nucleation time versus $1/h$ in the $q = 3$ Potts model, $h > 0$.

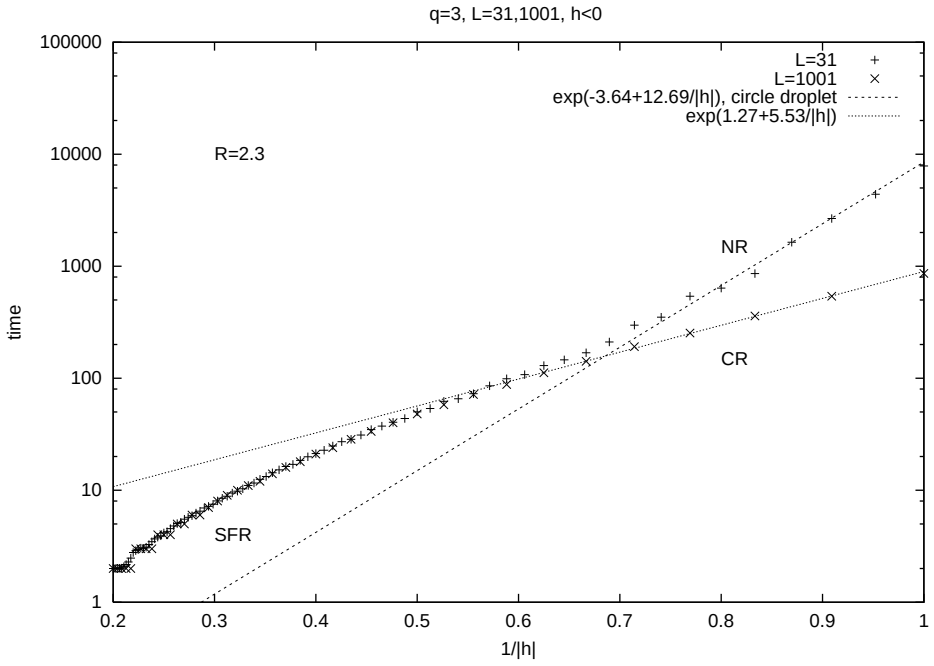



Figure 7: Nucleation time plotted against $1/|h|$ in the $q = 3$ Potts model, $h < 0$.

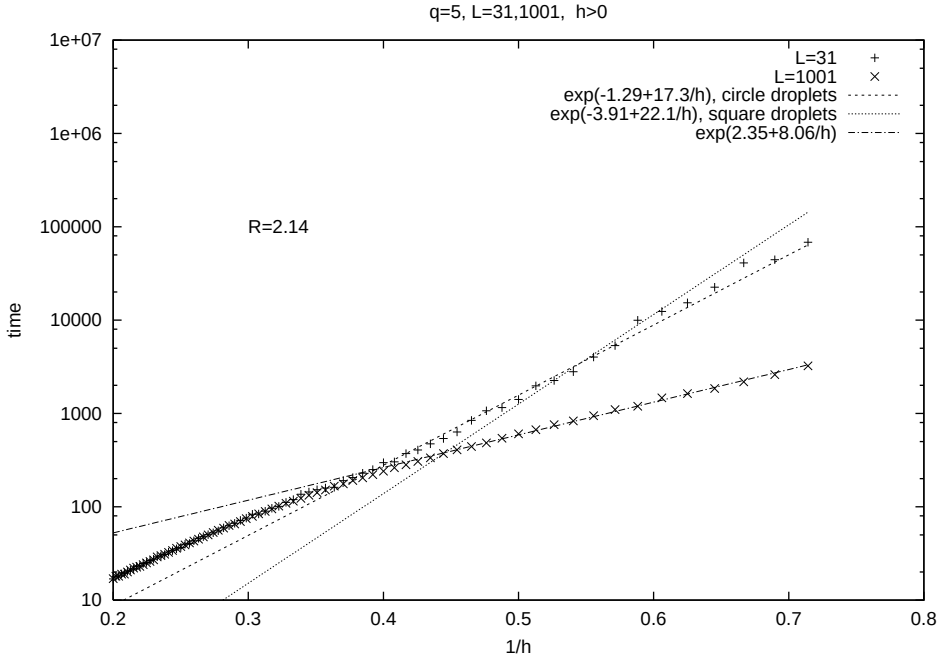



Figure 8: Nucleation time plotted against $1/h$ in the $q = 5$ Potts model, $h > 0$.

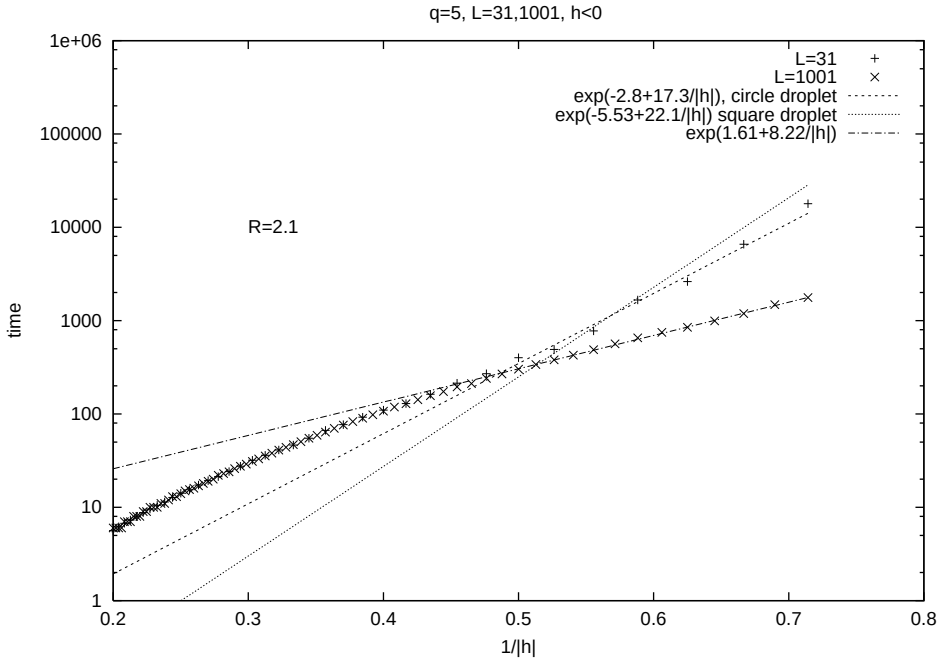



Figure 9: Nucleation time plotted against $1/|h|$ in the $q = 5$ Potts model, $h < 0$.

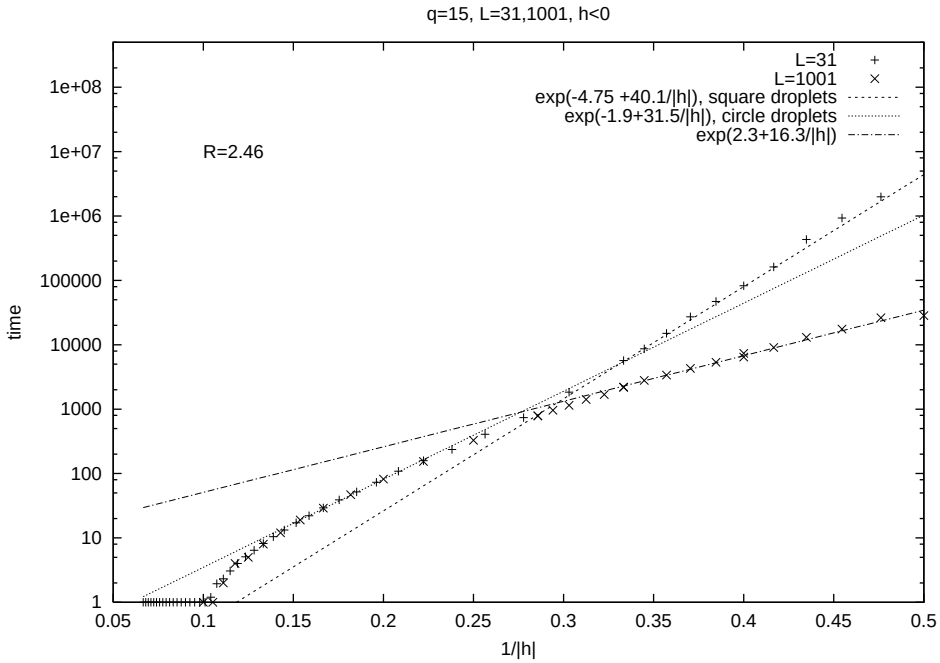



Figure 10: Nucleation time plotted against $1/|h|$ in the $q = 15$ Potts model, $h < 0$.